Bilayer Membranes of Triple-Chain Ammonium Amphiphiles

Toyoki Kunitake,* Nobuo Kimizuka, Nobuyuki Higashi, and Naotoshi Nakashima

Contribution No. 706 from the Department of Organic Synthesis, Faculty of Engineering, Kyushu University, Fukuoka, 812 Japan. *Received August 31, 1983*

Abstract: Ten ammonium amphiphiles which possess three long-chain alkyl tails (C_{12} or C_{16}) were prepared. They form clear aqueous dispersions upon sonication. Electron microscopy and light scattering experiments indicated the formation of huge bilayer aggregates except for one case. These bilayers undergo the characteristic crystal-to-liquid crystal-phase transition, as confirmed by differential scanning calorimetry (DSC) and by fluorescence depolarization of a diphenylhexatriene probe. Riboflavin, a water-soluble fluorescent probe, was shown to be trapped in bilayer vesicles of some triple-chain amphiphiles. Mixing of these bilayers with those of single-chain and double-chain amphiphiles was examined by DSC and by absorption spectroscopy. Together with our previous results, the present study establishes that the bilayer formation is a general phenomenon that is observable for a wide variety of synthetic amphiphiles.

Ammonium amphiphiles of single alkyl chains form fluid micelles in water, but those of double alkyl chains form stable bilayer membranes.[1] What happens with triple-chain ammonium amphiphiles? We reported in a previous publication[2] that trioctylmethylammonium chloride (**1**), a representative phase-transfer catalyst, produced relatively small (MW < 10^4), tight aggregates in water. This aggregate provides catalytic sites more hydrophobic than those obtained from conventional surfactant micelles. The reason why **1** does not form a better organized aggregate is probably that the alkyl chain (C_8) is too short. In the case of double-chain ammonium amphiphiles, the bilayer assembly is not formed unless the alkyl chain is longer than C_8.[3] Therefore, in a subsequent, preliminary study, we prepared aqueous dispersions of tridodecylmethylammonium bromide **2** (n = 12) in the hope that the bilayer aggregate is present. Unfortunately, however, we could not find any evidence of bilayer formation. The alkyl chain length per se should have been sufficient for bilayer assemblage, since aqueous bilayers are obtainable from didodecyldimethylammonium bromide.[1]

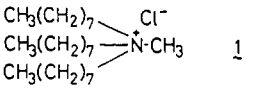

1

We showed previously that single-chain amphiphiles with rigid aromatic segments give rise to the bilayer assembly.[4-7] Apparently, the improved molecular orientation due to the rigid segment is crucial for bilayer formation. If this is the case, amphiphiles with three, *oriented* alkyl chains would be able to produce the bilayer structure. This type of bilayer assemblage would be interesting, especially because there is no counterpart in the biolipid.

In the present study, we prepared a series of triple-chain ammonium amphiphiles and examined their aggregation behavior. The results establish that the bilayer membrane is in fact formed from triple-chain amphiphiles. The triple-chain amphiphiles used are shown in Chart I.

Chart I

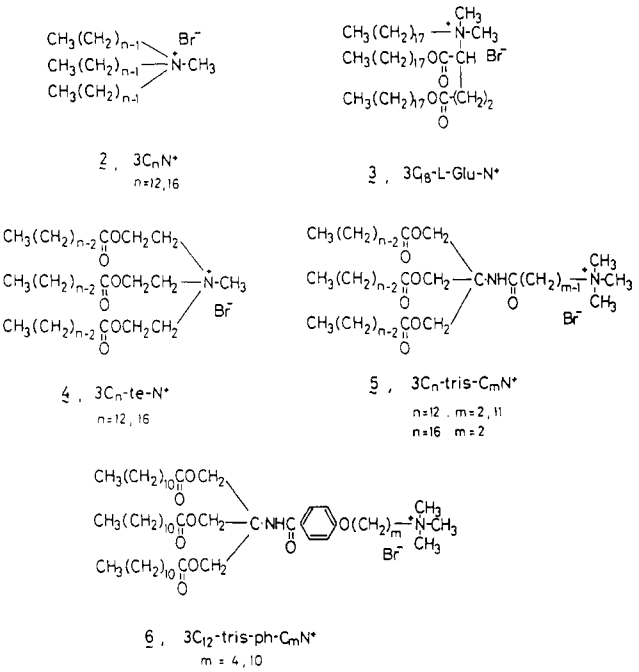

2, $3C_nN^+$, n=12,16

3, $3C_8$-L-Glu-N^+

4, $3C_n$-te-N^+, n=12, 16

5, $3C_n$-tris-C_mN^+, n=12, m=2, 11; n=16, m=2

6, $3C_{12}$-tris-ph-C_mN^+, m = 4, 10

Experimental Section

Preparation of Trialkylmethylammonium Bromide ($3C_nN^+$; n = 12, 16). Dodecylamine (10 g, 0.054 mol) and 43 g (0.17 mol) of dodecyl bromide were dissolved in 200 mL of ethanol and refluxed for 6 days in the presence of excess Na_2CO_3 (44 g). The inorganic salts were separated, and unreacted materials were removed in vacuo. The residual yellow oil was dissolved in ethyl acetate, crystallized in a freezer, and washed quickly with methanol to give low-melting solids, yield 22.6%. Tridodecylamine thus obtained (5 g, 0.012 mol) was dissolved in 50 mL of ethanol and allowed to react with 10 mL (0.18 mol) of CH_3Br in an ampule for 183 h at 90–95 °C. The solvent was removed and the residual oil crystallized in ethyl acetate: $3C_{12}N^+$, yield 3.7 g (52%) after recrystallization from ethyl acetate, mp 70–83 °C. The final structure was confirmed by IR and NMR spectroscopies: NMR ($CDCl_3$) δ 3.38 (s, 3, N^+–CH_3), 3.57 (s, 6, N^+-CH_2). Anal. Calcd for $C_{37}H_{78}NBr$: C, 72.03; H, 12.74; N, 2.27. Found: C, 71.87; H, 12.88; N, 2.30.

$3C_{16}N^+$ was prepared with similar procedures by reaction of hexadecylamine and hexadecyl bromide accompanied by quaternization: colorless powder; mp 79–80.5 °C; NMR ($CDCl_3$) δ 3.33 (s, 3, N^+–CH_3), 3.51 (s, 6, N^+–CH_2). Anal. Calcd for $C_{49}H_{102}NBr\cdot H_2O$: C, 73.27; H, 13.05; N, 1.74. Found: C, 73.50; H, 13.11; N, 1.76. The presence of water of hydration was supported by a broad IR peak at 3450 cm^{-1}.

Dioctadecyl *N*,*N*-Dimethyl-*N*-octadecyl-L-glutamate ($3C_{18}$-Glu-N^+). Dioctadecyl *N*,*N*-dimethylglutamate hydrochloride (mp 84–85 °C; 3.2 g, 0.0046 mol)[8] was treated with aqueous Na_2CO_3. The diester was then mixed with 15.2 g (0.046 mol) of octadecyl bromide in dimethylformamide and allowed to react for 10 days at 50–60 °C. The product was

(1) Kunitake, T.; Okahata, Y. *J. Am. Chem. Soc.* **1977**, *97*, 3860–3861 and subsequent publications.
(2) Okahata, Y.; Ando, R.; Kunitake, T. *J. Am. Chem. Soc.* **1977**, *99*, 3067–3072.
(3) Kunitake, T.; Okahata, Y.; Tamaki, K.; Kumamaru, F.; Takayanagi, M. *Chem. Lett.* **1977**, 387–390.
(4) Kunitake, T.; Okahata, Y. *J. Am. Chem. Soc.* **1980**, *102*, 549–553.
(5) Okahata, Y.; Kunitake, T. *Ber. Bunsenges. Phys. Chem.* **1980**, *84*, 550–556.
(6) Okahata, Y.; Ihara, H.; Shimomura, M.; Tawaki, S.; Kunitake, T. *Chem. Lett.* **1980**, 1169–1172.
(7) Kunitake, T.; Okahata, Y.; Shimomura, M.; Yasunami, S.; Takarabe, K. *J. Am. Chem. Soc.* **1981**, *103*, 5401–5413.
(8) Kunitake, T.; Nakashima, N.; Hayashida, S.; Yonemori, K. *Chem. Lett.* **1979**, 1413–1416.

0002-7863/84/1506-1978$01.50/0

recovered by adding hexane and ethyl acetate and then recrystallized from a mixture of hexane, ethyl acetate, and acetone and from ethanol giving a colorless powder: yield 5.2%; mp 87–87.5 °C. NMR and IR spectra were consistent with the structure: NMR ($CDCl_3$) δ 3.50 (s, 6, N^+–CH_3), 3.60 (s, 3, N^+–CH_2, N^+–CH). Anal. Calcd for $C_{61}H_{128}O_4NBr$: C, 71.86; H, 12.65; N, 1.37. Found: C, 72.19; H, 11.88; N, 1.43.

***O,O',O''*-Trialkanoyl-*N*-methyltriethanolamine Bromides ($3C_n$-te-N^+; *n* = 12,16).** Chloroform solutions (100 mL) of 0.14 mol of dodecanoyl chloride (30.6 g) or hexadecanoyl chloride (38.5 g) were added with stirring to chloroform solutions (100 mL) of 4.0 g (0.027 mol) of triethanolamine and 14.5 g (0.14 mol) of triethylamine in an ice bath. Upon further stirring at room temperature for 20 h, the mixtures were washed and dried. The solvent was removed and colorless crystals were collected. The product triesters were quaternized with CH_3Br in benzene in sealed ampules at 50 °C for 1 week. Benzene was removed and the residual viscous oil was recrystallized from ethyl acetate. $3C_{12}$-te-N^+: yield 53%; mp 147 °C; NMR ($CDCl_3$) δ 3.43 (s, 3, N^+–CH_3), 4.62 (s, 6, O–CH_2). Anal. Calcd for $C_{43}H_{84}O_6NBr{\cdot}0.5H_2O$: C, 64.55; H, 10.71; N, 1.75. Found: C, 64.57; H, 10.70; N, 1.68. $3C_{16}$-te-N^+: yield 50%; mp 103–105 °C; NMR ($CDCl_3$) δ 3.61 (s, 3, N^+–CH_3), 4.63 (s, 6, O–CH_2). Anal. Calcd for $C_{55}H_{108}O_6NBr$: C, 68.86; H, 11.35; N, 1.46. Found: C, 68.94; H, 11.41; N, 1.41.

***O,O',O''*-Trialkanoyl-*N*-((trimethylammonio)acetyl)tris(hydroxymethyl)aminomethane Bromides ($3C_n$-tris-C_2N^+; *n* = 12, 16) and *O,O',O''*-Tridodecanoyl-*N*-((ω-trimethylammonio)dodecanoyl)tris(hydroxymethyl)aminomethane Bromide ($3C_{12}$-tris-$C_{11}N^+$).** Tris(hydroxymethyl)aminomethane (3.8 g, 0.031 mol), 9.0 g (0.048 mol) of *p*-toluenesulfonic acid, and 0.13 mol of hexadecanoic acid (33.3 g) or dodecanoic acid (25.4 g) were dissolved in toluene, and water was removed as an azeotropic mixture with a Dean–Stark trap. The reactions were continued until stoichiometric amounts of water were recovered. Toluene was removed and the precipitates were recrystallized from acetonitrile and ether. The product triesters were identified by IR and NMR spectra. To THF solutions of 0.012 mol of the triesters and 0.024 mol of triethylamine were dropwise added to solutions of ω-bromoalkanoyl chlorides (0.024 mol) in dry THF, and the mixtures were stirred for 24 h at room temperature. THF was removed and the residues were recrystallized from methanol or ether to give colorless powders (yield 40–50%). Quaternization with trimethylamine was carried out as described above (room temperature, in benzene, 3–4 days), and after removal of excess trimethylamine and benzene, the residues were recrystallized 2 times from ethyl acetate or acetone. $3C_{16}$-tris-C_2N^+: colorless powder; yield 78%; mp 92–93.6 °C; NMR ($CDCl_3$) δ 3.51 (s, 9, N^+–CH_3), 4.45 (s, 6, O–CH_2). Anal. Calcd for $C_{57}H_{111}O_7N_2Cl{\cdot}1.5H_2O$: C, 68.53; H, 11.50; N, 2.80. Found: C, 68.33; H, 11.31; N, 2.80. $3C_{12}$-tris-C_2N^+: pale tan wax; yield 85%; mp 84.5–86.0 °C; NMR ($CDCl_3$) δ 3.48 (s, 9, N^+–CH_3), 4.50 (s, 6, O–CH_2). Anal. Calcd for $C_{45}H_{87}O_7N_2Cl{\cdot}0.5H_2O$: C, 66.51; H, 10.91; N, 3.45. Found: C, 66.24; H, 10.74; N, 3.46. $3C_{12}$-tris-$C_{11}N^+$: colorless powder; yield 54%; mp 89–89.6 °C; NMR ($CDCl_3$) δ 3.40 (s, 9, N^+–CH_3), 4.42 (s, 6, O–CH_2). Anal. Calcd for $C_{54}H_{105}O_7N_2Br{\cdot}0.5H_2O$: C, 65.96; H, 10.87; N, 2.85. Found: C, 65.71; H, 10.80; N, 2.86.

***O,O',O''*-Tridodecanoyl-*N*-[*p*-((ω-trimethylammonio)alkyloxy)benzoyl]tris(hydroxymethyl)aminomethane Bromide ($3C_{12}$-tris-ph-C_mN^+; *m* = 4, 10).** *p*-(ω-Bromobutyloxy)benzoic acid, bp 160–162 °C (0.03 mmHg), and *p*-(ω-bromodecyloxy)benzoic acid, bp 200–205 °C (0.001 mmHg), were refluxed in excess $SOCl_2$ for 5–7 h and excess $SOCl_2$ was removed in vacuo. The residual solids were taken up in dry THF and added dropwise with ice cooling to dry THF solutions of the tosylate salt of *O,O',O''*-tridecanoyltris(hydroxymethyl)aminomethane (see above) which had been neutralized with triethylamine. The mixtures were stirred at room temperature for 24 h, and triethylamine hydrochloride was separated. Colorless waxes obtained upon removal of THF were recrystallized from ethanol (yield 60%). The formation of the amide products was confirmed by IR and NMR spectroscopies. The quaternization with trimethylamine was conducted as described above. The products were recrystallized from acetone and from acetone/ethyl acetate to give colorless powders in yields of 50–60%. C_{12}-tris-ph-C_4N^+: mp 158–159 °C; NMR ($CDCl_3$) δ 3.50 (s, 9, N^+–CH_3), 4.59 (s, 6, O–CH_2). Anal. Calcd for $C_{54}H_{97}O_2N_2Br$: C, 66.03; H, 9.95; N, 2.85. Found: C, 65.78; H, 9.99; N, 2.83. $3C_{12}$-tris-ph-$C_{10}N^+$: mp 58–59 °C; NMR ($CDCl_3$) δ 3.47 (s, 9, N^+–CH_3), 4.67 (s, 6, O–CH_2). Anal. Calcd for $C_{60}H_{109}O_8N_2Br{\cdot}1.5H_2O$: C, 65.91; H, 10.32; N, 2.56. Found: C, 65.73; H, 10.21; N, 2.63.

Measurements. Aqueous solutions of triple-chain amphiphiles were prepared by sonication with a Branson Sonifier 185 (microtip, sonic power 40). The critical micelle (aggregate) concentration (cmc) was determined by the conductivity measurement of aqueous amphiphiles in the concentration range 1×10^{-6} to 2×10^{-4} M at 25 °C. The plots of specific conductivity (in $\mu S{\cdot}cm^{-1}$) against amphiphile concentration gave breaks which correspond to the cmc. Electron microscopy (Hitachi H-600 electron microscope) was carried out for negatively stained samples as described previously.[4] The aggregate weight was obtained by a small-angle light-scattering apparatus with the He–Ne laser light source (Toyo Soda, LS-8).[7] Differential scanning calorimetry (Daini-Seikosha, SSC/560) was conducted for 20-mM samples. The temperature was raised from 0 °C at a rate of 2 °C/min. The details are given elsewhere.[9]

Table I. Aggregation Behavior

	10^5-cmc, M	aggregate wt, 10^6 dalton	electron micrograph
$3C_{12}N^+$	3.8	240	no structure
$3C_{16}N^+$	1.3	23	partial vesicle and lamella
$3C_{12}$-te-N^+	2.4	38	vesicle and lamella (layers unclear)
$3C_{16}$-te-N^+	1.8	99	fragmentary lamella
$3C_{18}$-L-Glu-N^+	0.9	12	lamella
$3C_{12}$-tris-C_2N^+	0.7	9	multiwalled vesicle
$3C_{16}$-tris-C_2N^+	0.6	27	multiwalled vesicle
$3C_{12}$-tris $C_{11}N^+$	1.0	13	single-walled vesicle
$3C_{12}$-tris-ph-C_4N^+	0.8	26	undulating lamella
$3C_{12}$-tris-ph-$C_{10}N^+$	0.7	36	thick lamella and vesicle

Probe Trapping and Fluorescence Depolarization. Aqueous solutions of amphiphiles (20 mM) containing 0.1 mM of riboflavin (Wako Pure Chemical, first grade) were obtained by sonication in deonized water. Upon aging for 30 min at room temperature, the solutions were subjected to gel chromatography with a Sephadex G 50 column. The emission intensity of riboflavin at 525 nm was determined for 1-mL fractions with a Hitachi 650-10S spectrofluorimeter (excitation wavelength 380 nm). The trapping efficiency was estimated from the elution profile. The degree of fluorescence polarization (*P*) was obtained by eq 1.

$$P = \frac{(I_{\parallel\parallel} - I_{\parallel\perp} I_{\perp\parallel})/I_{\perp\perp}}{(I_{\parallel\parallel} + I_{\parallel\perp} I_{\perp\parallel})/I_{\perp\perp}} \quad (1)$$

A stock solution (1.0×10^{-3} M) of 1,6-diphenyl-1,3,5-hexatriene (DPH, Tokyo Kasei, special grade) was prepared in THF. A small portion (5 μL) of the stock solution was, after solvent removal, added with aqueous dispersions (5 mL) of amphiphiles, and the mixture was lightly sonicated. The fluorescence spectra were measured as described above: excitation at 360 nm, and emission maximum at 430 nm.

Results and Discussion

Aggregation Behavior. The aggregation behavior of the triple-chain amphiphiles is summarized in Table I. They all give clear aqueous solutions upon sonication. The cmc values as determined by the conductivity method are close to 1×10^{-5} M in most cases. This value is also close to those of typical, bilayer-forming double-chain ammonium amphiphiles. The cmc values of $2C_{12}N^+2C_1Br^-$ and $2C_{18}N^+2C_1Br^-$ have been reported to be 5×10^{-5} M[10] and 0.5×10^{-5} M,[11] respectively. The number of alkyl chains (three vs. two) does not affect the cmc value much. The influence of the alkyl chain length is smaller among the triple-chain amphiphiles than among the double-chain amphiphiles. The cmc values of $3C_{12}N^+$ and $3C_{16}N^+$ and of $3C_{12}$-te-N^+ and $3C_{16}$-te-N^+ are quite close, and those of $3C_{12}$-tris-C_2N^+ and $3C_{16}$-tris-C_2N^+ are virtually the same.

The apparent molecular weights of the aggregate are extraordinarily large. They are in the range of 10^7–10^8 daltons. Huge aggregate weights such as these are commonly observed in the bilayer system. The double-chain ammonium amphiphiles $2C_nN^+2C_1$ (*n* = 12, 18) give aggregate weights of 10^6–10^7 dal-

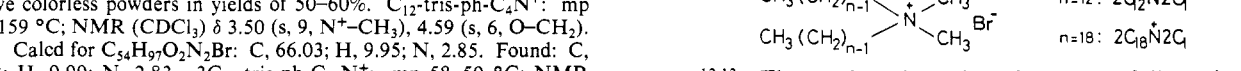

tons.[12,13] These values depend on the extent of dispersion (by

(9) Okahata, Y.; Ando, R.; Kunitake, T. *Ber. Bunsenges. Phys. Chem.* **1981**, *85*, 789–798.
(10) Ralston, A. W.; Eggenberger, D. N.; Dubrow, P. L. *J. Am. Chem. Soc.* **1948**, *70*, 977–979.
(11) Kunieda, H.; Shinoda, K. *J. Phys. Chem.* **1978**, *82*, 1710–1714.
(12) Okahata, Y.; Ando, R.; Kinitake, T. *Bull. Chem. Soc. Jpn.* **1979**, *52*, 3647–3653.

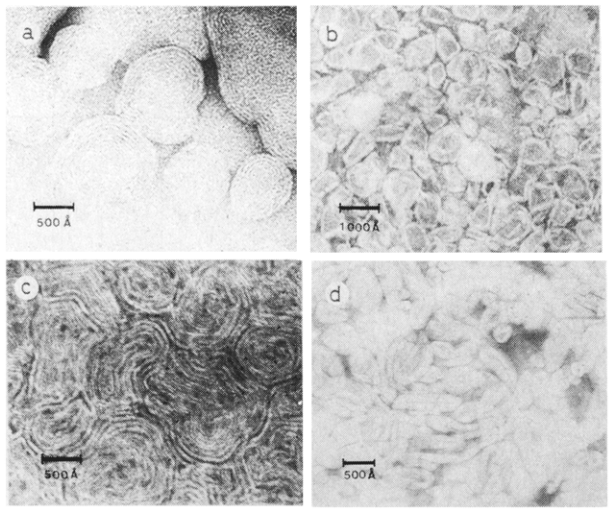

Figure 1. Electron micrograph of triple-chain amphiphiles stained by uranyl acetate: (a) $3C_{12}$-tris-C_2N^+, original magnification ×50 000; (b) $3C_{12}$-tris-$C_{11}N^+$, original magnification ×30 000; (c) $3C_{12}$-tris-ph-C_4N^+, original magnification ×50 000; (d) $3C_{12}$-tris-ph-$C_{10}N^+$, original magnification ×40 000.

sonication), and therefore, detailed comparisons are avoided. In spite of this limitation it can be said that the triple-chain amphiphiles give aggregates larger than those of the related double-chain amphiphiles. Again, we cannot find among triple-chain amphiphiles definite relations between the alkyl chain length and the aggregation number.

Electron microscopy provides strongest evidence for bilayer formation. The bilayer structure was observed for all the triple-chain amphiphiles except for $3C_{12}N^+$. The development of the bilayer structure appears limited in the case of $3C_{16}N^+$ and $3C_{12}$-te-N^+. $3C_{16}$-te-N^+ produces clearer bilayer structures. The tris connector is quite effective for formation of well-developed bilayers, and all five of the triple-chain compounds with this connector show definite bilayer structures in electron micrographs. Examples are illustrated in Figure 1. $3C_{12}$-tris-C_2N^+ produces aggregates of multiwalled vesicles (layer width 60–70 Å), as shown in Figure 1a. $3C_{16}$-tris-C_2N^+ gives similar aggregates. In contrast, well-developed single-walled vesicles are obtainable from $3C_{12}$-tris-$C_{11}N^+$ (Figure 1b). Strangely, these vesicles do not have uniform surface curvature. The molecular packing must become irregular at certain areas of this bilayer. The aggregate morphology of $3C_{12}$-tris-ph-C_4N^+ is undulating lamellae, and that of $3C_{12}$-tris-ph-$C_{11}N^+$ is thick lamellae and vesicles (Figure 1, parts c and d, respectively).

The structural element of the triple-chain amphiphile comprises the alkyl tail, connector portion, spacer portion, and hydrophilic head. The amphiphiles of Figure 1 are identical in the C_{12} tail, the tris connector, and the trimethylammonium head. The only difference are in the spacer portion. The influence of the spacer structure on the aggregate morphology is unexpectedly large.

The importance of the connector in giving well-developed bilayers may be inferred from the molecular model of representative amphiphiles. Figure 2 illustrates CPK molecular models of $3C_{12}N^+$, $3C_{12}$-te-N^+, and $3C_{12}$-tris-C_2N^+. In the case of $3C_{12}N^+$, the N–CH_3 is directed away from the three C_{12} chains. The long chains cannot be aligned snugly at locations close to the ammonium head because of the tetrahedral configuration of the ammonium group. In contrast, the alkyl chains of $3C_{12}$-te-N^+ can be aligned nicely as shown in Figure 2b. The compact packing in this case is produced by the presence of the ester unit, and the ammonium head can stick out without conformational constraint. The same situation is found for $3C_{12}$-tris-C_2N^+ (Figure 2c), again due to the presence of the ester linkage. The hydrophilic head, however, is recognizable more distinctly, because the spacer portion is present.

(13) Herrmann, U.; Fendler, J. H. *Chem. Phys. Lett.* **1979**, *64*, 270–274.

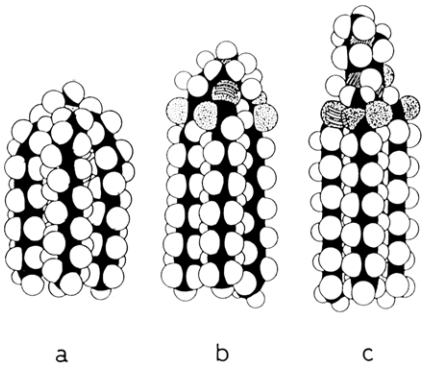

Figure 2. CPK molecular models of triple-chain amphiphiles with different connectors: (a) $3C_{12}N^+$, (b) $3C_{12}$-te-N^+, (c) $3C_{12}$-tris-C_2N^+.

Table II. Phase Transition Behavior

amphiphile	T_c, °C(ΔH, kcal/mol) sonicated sample	T_c, °C(ΔH, kcal/mol) frozen sample	inflection region,[a] °C
$3C_{12}N^+$	not detected	31.0 (15.2)	not detected
$3C_{16}N^+$	48.6[b] (8.8) 60.0	45.2 61.5[b] (26.0)	43, 60
$3C_{12}$-te-N^+	37.0 41.5[b] (1.1)	38.8 43.0[b] (10.3)	38
$3C_{16}$-te-N^+	60.5 (13.4)	63.3 (15.5)	63
$3C_{18}$-L-Glu-N^+	59.0 (12.5)	58.5 (15.9)	
$3C_{12}$-tris-C_2N^+	28.7 (2.4)	31.5 (7.4)	31
$3C_{16}$-tris-C_2N^+	45.0 61.5[b] (10.5)	63.5 (13.4)	62
$3C_{12}$-tris-$C_{10}N^+$	41.5 (7.6)	59.0 (24.6)	41
$3C_{12}$-tris-ph-C_4N^+	20.1 (2.7)	21.5 (7.6)	
$3C_{12}$-tris-ph-$C_{10}N^+$	51.5 (8.0)	51.7 (13.3)	

[a] Fluorescence polarization of DPH. [b] Major peak.

It is evident from a comparison of the three CPK models that the tris and te (triethanolamine) connectors facilitate the orientation of alkyl tails, leading to formation of the two-dimensional molecular array.

Phase Transition. Aqueous bilayer membranes usually show the crystal-to-liquid crystal-phase transition. This phenomenon is readily observed by differential scanning calorimetry (DSC). We have made an extensive DSC study on the phase transition behavior of aqueous bilayers of synthetic, double-chain amphiphiles.[9] Table II summarizes the DSC data of the triple-chain amphiphiles. A sonicated sample of $3C_{12}N^+$ does not show any DSC peak in the temperature range studied, (0–100 °C), but the corresponding frozen sample gives a peak at 31 °C. This implies that the regular bilayer structure is not formed for the sonicated sample of $3C_{12}N^+$, in accordance to the electron microscopic observation.

All the other triple-chain amphiphiles showed phase transition peaks regardless of whether sample solutions were sonicated at room temperature or frozen at −50 °C. The peaks for the two kinds of the samples are located at almost the identical temperatures except for $3C_{12}$-tris-$C_{11}N^+$. The phase transition temperature (T_c) is elevated by elongation of the alkyl tail (e.g., $3C_{12}$-te-N^+ vs. $3C_{16}$-te-N^+) and by the presence of a long spacer (e.g., $3C_{12}$-tris-C_2N^+ vs. $3C_{12}$-tris-$C_{11}N^+$). Transition enthalpies (ΔH) of the sonicated samples are in most cases small for amphiphiles of the C_{12} tail. ΔH is greater for a frozen sample than for the corresponding sonicated sample.

Different DSC behaviors have been observed for sonicated and frozen samples of aqueous bilayer dispersions of some double-chain amphiphiles, and the differences in T_c and ΔH are attributed to formation of lyotropic liquid-crystalline phases in the frozen sample.[9] The discrepancy was found usually for simple cationic and anionic double-chain compounds, but was not recognizable for zwitterionic and nonionic double-chain amphiphiles. Double-chain ammonium amphiphiles with enhanced intermolecular interaction (improved molecular alignment) similarly do not show

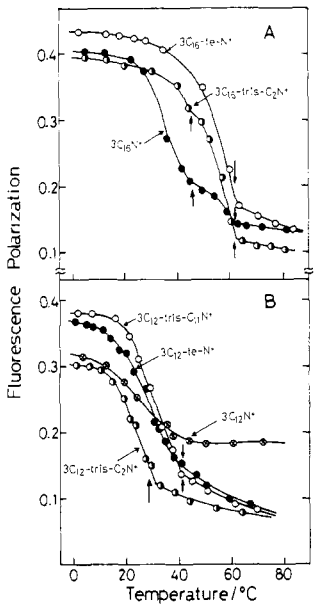

Figure 3. Temperature dependence of fluorescence polarization of DPH in bilayer matrices of triple-chain amphiphiles ([amphiphile] = 1×10^{-3} M, [DPH] = 1×10^{-6} M): (A) amphiphiles with C_{16} tails, (B) amphiphiles with C_{12} tails. The arrows indicate the peak-top temperature (T_c) in the DSC thermogram.

the discrepancy. Similar situations are found for the DSC behavior of the triple-chain ammonium amphiphiles. Thus, the T_c discrepancy is observed for $3C_{12}N^+$ and $3C_{16}N^+$ but not (or very small ones) for the other amphiphiles. In the latter cases, the tris and te connectors (ester unit) seem to stabilize particular molecular arrangements which are maintained in sonicated and frozen samples.

The phase transition behavior may be examined also by fluorescence polarization of 1,6-diphenyl-1,3,5-hexatriene (DPH) bound to the bilayer matrix. Application of this technique to the bilayer membrane of double-chain ammonium salts has been described elsewhere.[14] In this case, fluorescence polarization P is large (0.3–0.4) when DPH is immobilized in the crystalline bilayer matrix and decreases to ca. 0.1 in the fluid (liquid-crystalline) bilayer.

Figure 3 shows the temperature dependence of P for the two tail series (C_{12} and C_{16} tails). In the case of $3C_{12}N^+$, P decreases gradually with temperature rise. This is consistent with the lack of specific T_c in the DSC study. The other members of the $3C_{12}$ amphiphile give more drastic decreases in P with temperature. The P values starts to decrease at temperatures about 20 °C below T_c, and inflections appear near T_c and keep decreasing beyond T_c. Therefore, the P variation cannot specify the location of the phase transition exactly, although the inflection regions are close to T_c (peak top temperature in the DSC data) as shown in Table II.

More definite correspondence is available with the $3C_{16}$ amphiphiles. $3C_{16}N^+$ shows two inflections, which correspond to the two DSC peaks. The inflection at the higher temperature exactly agrees with T_c, and P changes little beyond that temperature. In the case of $3C_{16}$-te-N^+ and $3C_{16}$-tris-C_2N^+, the inflection temperatures are quite close to T_c.

Both the DSC and polarization data prove beyond doubt that the triple-chain amphiphile produces typical bilayer aggregates.

Excimer Formation. Double-chain ammonium amphiphiles with the benzene ring in the spacer portion, **8**, give rise to excimer

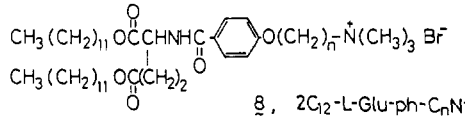

8, $2C_{12}$-L-Glu-ph-C_nN^+

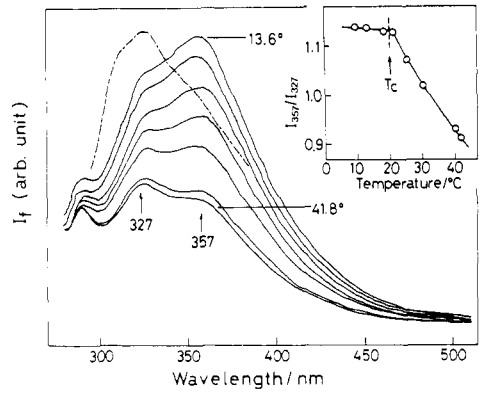

Figure 4. Temperature dependence of fluorescence spectra of the aqueous $3C_{12}$-tris-ph-C_4N^+ bilayer (excitation wavelength 265 nm): (solid line) $3C_{12}$-tris-ph-C_4N^+, 1.0×10^{-4} M; (dotted line) $3C_{12}$-tris-ph-C_4N^+, 1.0×10^{-4} M and CTAC, 1.0×10^{-2} M at 14 °C. Insert shows the variation of the relative fluorescence intensity at 357 and 327 nm.

emission in the bilayer assembly.[15] Monomer and excimer fluorescences were observed for the liquid-crystalline bilayer, and the excimer emission becomes absent upon phase transition to the crystalline bilayer.

The same situation may arise for the bilayer aggregate of triple-chain amphiphiles. Figure 4 illustrates the variation of fluorescence spectra of aqueous $3C_{12}$-tris-ph-C_4N^+ bilayers. At ca. 40 °C, the spectrum consists of two peaks at 327 (main) and 357 nm. With increasing temperature, the relative fluorescence intensity of the two peaks is reversed. The peak at 357 nm disappears upon addition of micellar CTAC (10 mM) at 14 °C. These spectral patterns are the same as those observed for the $2C_{12}$-L-Glu-ph-C_4N^+ bilayer, and the two peaks at 357 and 327 nm are attributed to the excimer and monomer emissions, respectively.

The insert in Figure 4 shows the temperature dependence of relative fluorescence intensity I_{357}/I_{327}. The variation is represented by two lines intersecting at a temperature close to T_c. The intensity ratio does not change at $T < T_c$ and decreases linearly at $T > T_c$. It is clear that the excimer emission is more efficient in the rigid bilayer matrix.

It has been indicated that the interplanar distance is 3.2 Å for typical excimer-forming pairs of the chromophore.[16] The data of Figure 4 indicate that the spatial arrangement of the two benzene chromophores is suitable for excimer formation in the crystalline bilayer. In the bilayer matrix of double-chain amphiphile $2C_{12}$-L-Glu-ph-C_4N^+, contrasting results are obtained: the excimer formation was prevailing in the liquid-crystalline state but not in the crystalline state. The molecular cross section of amphiphiles in the bilayer assembly is usually greater in the liquid-crystalline state than in the crystalline state. Therefore, it is suggested that the expanded cross section of the double-chain amphiphile produces the chromophore distance (and/or orientation) which is favorable for excimer formation. The molecular cross section of the triple-chain component is naturally greater than that of the double-chain counterpart. Then, the chromophore distance may as well be suited for the excimer formation even in the crystalline state. This explanation is not inconsistent with the fact that the excimer emission is observed at all temperatures for the bilayer of a double-chain fluorocarbon amphiphile, $2C^F_{10}$-L-Glu-ph-C_4N^+.[15] Apparently, the cross section of this amphiphile

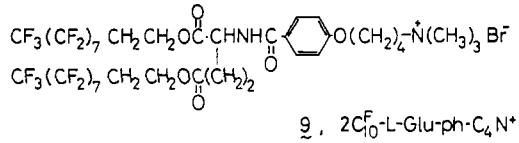

9, $2C^F_{10}$-L-Glu-ph-C_4N^+

(14) Nagamura, T.; Mihara, S.; Okahata, Y.; Kunitake, T.; Matsuo, T. *Ber. Bunsenges. Phys. Chem.* **1978**, *82*, 1093–1098.

(15) Kunitake, T.; Tawaki, S.; Nakashima, N. *Bull. Chem. Soc. Jpn.* **1983**, *56*, 3235–3242.

(16) Klöpffer, W. "Organic Molecular Photophysics"; Birks, J. B., Ed.; Wiley-Interscience: New York, 1973; Vol. 1, Chapter 7.

Table III. Riboflavin Trapping

membrane	% of bound riboflavin	fluorescence polarization (P): membrane matrix	fluorescence polarization (P): bulk phase
$3C_{12}$-tris-C_2N^+	1.5	0.22	0.012
$3C_{16}$-tris-C_2N^+	1.9	0.28	
$3C_{12}$-tris-$C_{11}N^+$	1.1	0.40	
$3C_{12}$-tris-ph-$C_{10}N^+$	1.8	0.48	

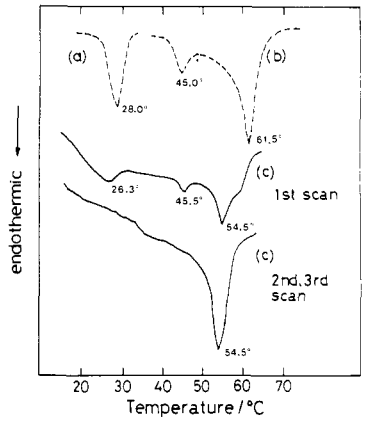

Figure 5. DSC thermograms (heating rate, 2.0 °C/min): (a) $2C_{16}N^+$-$2C_1$, 10 mM; (b) $3C_{16}$-tris-C_2N^+, 10 mM; (c) an equimolar mixture (5 mM each) of $2C_{16}N^+2C_1$ and $3C_{16}$-tris-C_2N^+.

produces the chromophore arrangement which is close to those of the crystalline bilayer of the triple-chain amphiphile and of the liquid-crystalline bilayer of the double-chain, hydrocarbon amphiphile.

Riboflavin Trapping. Riboflavin is a convenient water-soluble probe for examining the trapping capability of bilayer vesicles.[17] Table III summarizes the results of the trapping experiment. The amount of bound riboflavin is 1–2%—the typical trapping efficiency observed for other bilayer vesicles. The aggregate morphology of the triple-chain amphiphiles of Table III are either single-walled or multiwalled vesicles. This may be related to the invariance of the trapping efficiency.

Fluorescence polarization P for trapped riboflavin is considerably greater than that in the bulk phase. This suggests that riboflavin molecules trapped in the vescile are immobilized near or at the bilayer surface. It is interesting in this respect that riboflavin bound to $3C_{12}$-tris-$C_{11}N^+$ and $3C_{12}$-tris-ph-$C_{10}N^+$ gives larger P values than that bound to $3C_{12}$-tris-C_2N^+ and $3C_{16}$-tris-C_2N^+. The difference seems to arise from the change in the spacer portion. Riboflavin molecules are immobilized probably deeper in the spacer portion in the former cases.

Riboflavin trapped in the vesicle of $2C_{12}$-L-Glu-ph-C_2N^+ gave $P = 0.35$. This is intermediate of the two separate P values (0.2–0.3 and 0.4–0.5) observed for the triple-chain amphiphiles, consistent with the intermediate spacer length of this double-chain amphiphile.

Membrane Mixing. The lipid bilayer of biomembranes is usually composed of a large variety of lipid components, and miscibility of these lipid molecules are directly related to the biomembrane function. The same situation arises for synthetic bilayer membranes, and miscibility or the lack of it (i.e., phase separation) has been examined in relation to the bilayer function.

The miscibility of triple-chain amphiphiles with other types of bilayer-forming amphiphiles was studied by DSC and absorption spectroscopy. Figure 5 shows DSC thermograms of the aqueous bilayer of dihexadecyldimethylammonium bromide ($2C_{16}N^+2C_1$) and $3C_{16}$-tris-C_2N^+, and their mixture. The alkyl tail of these compounds is approximately of the same length. When separately

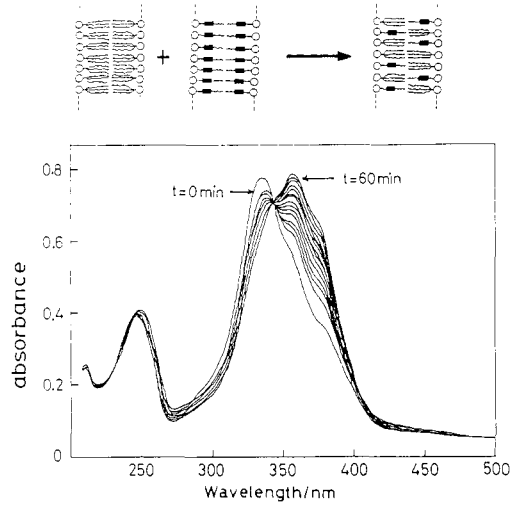

Figure 6. Spectral change due to membrane mixing. $[3C_{12}$-tris-$C_{11}N^+]$ = 5.0×10^{-4} M; $[C_{12}AzoC_{10}N^+]$ = 5.0×10^{-5} M; 48 °C.

Table IV. Membrane-Forming Amphiphiles

type of amphiphile	illustrative molecular structure[a]	type of membrane	tail	ref (representative)
single chain		bilayer	hydrocarbon	7
		bilayer	fluorocarbon	20
		monolayer	hydrocarbon	19, 21
double chain		bilayer	hydrocarbon	1
		bilayer	fluorocarbon	20
triple chain		bilayer	hydrocarbon	this study
		bilayer	fluorocarbon	22
others		monolayer	hydrocarbon	23
		monolayer	hydrocarbon	24
polymeric	large variety		hydrocarbon	23, 25–29

[a] (Circle) hydrophilic head, (wave line) alkyl or fluoroalkyl chain, (rectangle) rigid segment.

measured, $2C_{16}N^+2C_1$ displays a phase transition peak at 28 °C (ΔH = 5.7 kcal/mol) and $3C_{16}$-tris-C_2N^+ at 45.0 and 61.5 °C (ΔH = 10.5 kcal/mol). In the first scan of the mixture, these three peaks are diminished and a new peak appears at 54.5 °C. Only the new peak (ΔH = 10.4 kcal/mol) remains upon further scans. This means that the two amphiphiles are completely mixed, giving rise to a new bilayer phase.

The miscibility with a single-chain amphiphile is readily estimated by using the spectral shift of the azobenzene chromophore. For instance, the bilayer aggregate of $C_{12}AzoC_{10}N^+$ possesses λ_{max} at 330 nm at room temperature. When aqueous triple-chain amphiphiles ($3C_{12}$-tris-$C_{11}N^+$ or $3C_{16}$-tris-C_2N^+; 10 times excess) are added, λ_{max} shifts to 357 nm. These results are very similar to that observed for mixing of the bilayers of $C_{12}AzoC_{10}N^+$ and $2C_{18}N^+2C_1$[18] and reflect dissolution of the $C_{12}AzoC_{10}N^+$ bilayer

(17) Kunitake, T.; Okahata, Y.; Yasunami, S. *Chem. Lett.* **1981**, 1397–1400.
(18) Shimomura, M.; Kunitake, T. *Chem. Lett.* **1981**, 1001–1004.
(19) Okahata, Y.; Kunitake, T. *J. Am. Chem. Soc.* **1979**, *101*, 5231–5234.
(20) Kunitake, T.; Okahata, Y.; Yasunami, S. *J. Am. Chem. Soc.* **1982**, *104*, 1285–1288.
(21) Baumgartner, E.; Fuhrhop, J. H. *Angew. Chem., Int. Ed. Engl.* **1980**, *19*, 550–551.
(22) Higashi, N., unpublished results in these laboratories.
(23) Kunitake, T.; Nakashima, N.; Takarabe, K.; Nagai, M.; Tsuge, A.; Yanagi, H. *J. Am. Chem. Soc.* **1981**, *103*, 5945–5947.
(24) Fuhrhop, J.-H.; Ellermann, K.; David, H. H.; Mathien, J. *Angew. Chem.* **1982**, *94*, 444–445.
(25) Hub, H. H.; Hupfer, B.; Koch, H.; Ringsdorf, H. *Angew. Chem.* **1980**, *92*, 962–964.
(26) Johnson, D. S.; Sanghera, S.; Pons, M.; Chapman, D. *Biochim. Biophys. Acta.* **1980**, *602*, 57–69.

into the bilayer matrix of triple-chain amphiphiles. Figure 6 is an example of the spectral change at 48 °C. The mixing is complete in ca. 1 h, because the $3C_{12}$-tris-$C_{11}N^+$ bilayer (T_c = 41.5 °C) is fluid at this temperature. The mixing rate becomes much smaller when the bilayers are in the crystalline state.

It is evident from the DSC and spectral results that the triple-chain amphiphiles show mixing behaviors very similar to those of double-chain (dialkyl) amphiphiles.

Amphiphile Structure and Bilayer Formation. In all aspects examined, triple-chain amphiphiles produce typical bilayer aggregates. Table IV summarizes types of synthetic amphiphiles which form molecular membranes (monolayer and bilayer). They are classified by the number of alkyl tails as single-chain, double-chain, triple-chain, related compounds, and the polymeric analogues. Single-chain amphiphiles are capable of forming a bilayer or monolayer, depending on the number of hydrophilic heads. They contain rigid segments and flexible tails as hydrophobic moieties. The flexible tail may be either hydrocarbon or fluorocarbon. Double-chain amphiphiles are composed of a variety of hydrophilic heads and flexible tails that are either hydrocarbon or fluorocarbon. They produce bilayers. Triple-chain amphiphiles are made of a hydrophilic head and three flexible tails of hydrocarbons or fluorocarbons and form bilayers. Other membrane-forming compounds include amphiphiles which are derived by connecting one of the alkyl tails of two double-chain amphiphiles. Further variations of membrane-forming amphiphiles are possible by combinations of these structural units. Polymeric and polymerized bilayers are yet another group of molecular membrane.

It is now established that formation of stable molecular membranes (monolayer and bilayer) is a general physicochemical phenomenon observed for a wide variety of amphiphiles. There have been proposed theories to account for self-assembly of surfactant molecules into micelles and vesicles. The original formulation of Tanford[30] was extended by Israelachvilli and others,[31] and, more recently, the quantitative aspects were discussed by Nagarajan and Ruckenstein[32] and by Mitchell and Ninham.[33] In these theories, however, the hydrophobic core is assumed to be liquid like, and the types of membrane-forming amphiphiles of Table IV may not be readily accommodated. It is evident that the improved molecular orientation and packing in the hydrophobic core promote the two-dimensional molecular assembly.

Acknowledgment. Financial support from Special Coordination Funds for Promoting Science and Technology (Science and Technology Agency of Japan) is gratefully acknowledged.

Registry No. 2 (n = 12), 29920-02-3; **2** (n = 16), 88932-02-9; **3**, 88932-05-2; **4** (n = 12), 88932-03-0; **4** (n = 16), 88932-04-1; **5** (m = 2; n = 12), 88932-06-3; **5** (m = 2; n = 16), 88932-07-4; **5** (m = 11; n = 12), 88932-08-5; **6** (m = 4), 88932-09-6; **6** (m = 10), 88932-10-9; $CH_3(CH_2)_{15}Br$, 112-82-3; $[CH_3(CH_2)_{10}C(O)O(CH_2)_2]_3N$, 3002-20-8; $[CH_3(CH_2)_{14}C(O)O(CH_2)_2]_3N$, 88931-91-3; $[CH_3(CH_2)_{10}C(O)OCH_2]_3CNH_2$, 88931-92-4; $[CH_3(CH_2)_{14}C(O)OCH_2]_3CNH_2$, 88931-93-5; $[CH_3(CH_2)_{10}C(O)OCH_2]_3CNHC(O)CH_2Br$, 88931-94-6; $[CH_3(CH_2)_{14}C(O)OCH_2]_3CNHC(O)CH_2Br$, 88931-95-7; HO_2C-p-$C_6H_4O(CH_2)_4Br$, 88931-96-8; HO_2C-p-$C_6H_4O(CH_2)_{10}Br$, 88931-97-9; $ClC(O)$-p-$C_6H_4O(CH_2)_4Br$, 88185-43-7; $ClC(O)$-p-$C_6H_4O(CH_2)_{10}Br$, 88931-98-0; $[CH_3(CH_2)_{10}C(O)OCH_2]_3CNH_2$·TsOH, 88931-99-1; $[CH_3(CH_2)_{10}C(O)OCH_2]_3CNHC(O)$-$p$-$C_6H_4O(CH_2)_4Br$, 88932-00-7; $[CH_3(CH_2)_{10}C(O)CH_2]_3NHC(O)$-$p$-$C_6H_4O(CH_2)_{10}Br$, 88932-01-8; $2C_{16}N^+2C_2Br^-$, 70755-47-4; $C_{12}AzoC_{10}N{\cdot}Br^-$, 88932-11-0; $[CH_3(CH_2)_{10}C(O)OCH_2]_3CNHC(O)(CH_2)_{10}CH_3$, 88932-12-1; dodecylamine, 124-22-1; dodecyl bromide, 143-15-7; tridodecylamine, 102-87-4; methyl bromide, 74-83-9; hexadecylamine, 143-27-1; dioctadecyl *N,N*-dimethylglutamate hydrochloride, 88931-89-9; dioctadecyl *N,N*-dimethylglutamate, 88931-90-2; octadecyl bromide, 112-89-0; dodecanoyl chloride, 112-16-3; hexadecanoyl chloride, 112-67-4; triethanolamine, 102-71-6; tris(hydroxymethyl)aminomethane, 77-86-1; hexadecanoic acid, 57-10-3; dodecanoic acid, 143-07-7; trimethylamine, 75-50-3; 1,6-diphenyl-1,3,5-hexatriene, 1720-32-7; riboflavin, 83-88-5.

(27) O'Brien, D. F.; Whitesides, T. H.; Klingbiel, R. T. *J. Polym. Sci., Polym. Lett. Ed.* **1981**, *19*, 95–101.
(28) Tundo, P.; Kippenberger, D. J.; Klahn, P. L.; Prieto, N. E.; Jao, T. C.; Fendler, J. H. *J. Am. Chem. Soc.* **1982**, *104*, 456–461.
(29) Regen, S. L.; Singh, A.; Oehme, G.; Singh, M. *J. Am. Chem. Soc.* **1982**, *104*, 791–795.
(30) Tanford, C. "The Hydrophobic Effect"; Wiley: New York, 1973.
(31) Israelachvilli, J. N.; Mitchell, D. J.; Ninham, B. W. *J. Chem. Soc., Faraday Trans. 2* **1976**, *72*, 1525–1568.
(32) Nagarajan, R.; Ruckenstein, E. *J. Colloid Interface Sci.* **1979**, *71*, 580–604.
(33) Mitchell, D. J.; Ninham, B. W. *J. Chem. Soc., Faraday Trans. 2* **1981**, *77*, 601–629.

Simple Method for Quantifying the Distribution of Organic Substrates between the Micellar and Aqueous Phases of Sodium Dodecyl Sulfate Solution[1]

T. J. Burkey,* D. Griller, D. A. Lindsay, and J. C. Scaiano

Contribution from the Division of Chemistry, National Research Council of Canada, Ottawa, Ontario, Canada K1A 0R6. *Received September 21, 1983. Revised Manuscript Received December 6, 1983*

Abstract: A simple technique, involving the measurement of diffusion coefficients, was used to determine partition coefficients for the distribution of a variety of organic substrates between the micellar and aqueous phases of sodium dodecyl sulfate (SDS) solution. The data additionally revealed two mechanisms for the apparent diffusion of the micelles. One involved true micellar diffusion and was monitored by the use of tracer molecules. The second involved a more rapid redistribution of micelles by a mechanism involving the diffusion of individual SDS molecules. Nonpolar molecules with more than 10 heavy atoms were essentially localized in the micellar phase of 0.1 M SDS.

There has been substantial interest in the use of micelles as devices for modifying chemical reactions.[2] In order to understand this chemistry, it is vital to known the extent to which an organic molecule is partitioned between the aqueous and micellar phases, yet there are few general methods for making such measurements since most require special spectral or other physical properties of the partitioned organic molecules.[3-6] Indeed, it is probably

(1) Issued as NRCC publication No. 23086.
(2) See, for example: Turro, N. J.; Weed, G. C. *J. Am. Chem. Soc.* **1983**, *105*, 1861 and references cited therein.
(3) Stiger, D.; Williams, R. J.; Mysels, K. J. *J. Phys. Chem.* **1955**, *59*, 330.

0002-7863/84/1506-1983$01.50/0 Published 1984 by the American Chemical Society